Journal of Virology®

AMERICAN SOCIETY FOR MICROBIOLOGY

# Age-Related Susceptibility of Ferrets to SARS-CoV-2 Infection

Mathias Martins,[a] Maureen H. V. Fernandes,[a] Lok R. Joshi,[a] Diego G. Diel[a]

aDepartment of Population Medicine and Diagnostic Sciences, College of Veterinary Medicine, Cornell University, Ithaca, New York, USA

**ABSTRACT** Susceptibility to severe acute respiratory syndrome coronavirus 2 (SARS-CoV-2) and the outcome of coronavirus disease 2019 (COVID-19) have been linked to underlying health conditions and the age of affected individuals. Here, we assessed the effect of age on SARS-CoV-2 infection using a ferret model. For this, young (6-month-old) and aged (18- to 39-month-old) ferrets were inoculated intranasally with various doses of SARS-CoV-2. By using infectious virus shedding in respiratory secretions and seroconversion, we estimated that the infectious dose of SARS-CoV-2 in aged animals is ~32 PFU per animal, while in young animals it was estimated to be ~100 PFU. We showed that viral replication in the upper respiratory tract and shedding in respiratory secretions is enhanced in aged ferrets compared to young animals. Similar to observations in humans, this was associated with higher transcription levels of two key viral entry factors, ACE2 and TMPRSS2, in the upper respiratory tract of aged ferrets.

**IMPORTANCE** In humans, ACE2 and TMPRSS2 are expressed in various cells and tissues, and differential expression has been described in young and old people, with a higher level of expressing cells being detected in the nasal brushing of older people than young individuals. We described the same pattern occurring in ferrets, and we demonstrated that age affects susceptibility of ferrets to SARS-CoV-2. Aged animals were more likely to get infected when exposed to lower infectious dose of the virus than young animals, and the viral replication in the upper respiratory tract and shedding are enhanced in aged ferrets. Together, these results suggest that the higher infectivity and enhanced ability of SARS-CoV-2 to replicate in aged individuals is associated, at least in part, with transcription levels of ACE2 and TMPRSS2 at the sites of virus entry. The young and aged ferret model developed here may represent a great platform to assess age-related differences in SARS-CoV-2 infection dynamics and replication.

**Keywords** SARS-CoV-2, COVID-19, ferrets, ACE2, TMPRSS2

In late December 2019, several cases of viral pneumonia of unknown etiology were described in a cluster of people in Wuhan, Hubei province, China. The causative virus severe acute respiratory syndrome coronavirus 2 (SARS-CoV-2), a new member of the family *Coronaviridae*, was subsequently discovered and the disease named coronavirus disease 19 (COVID-19) (1). Since the description of the first cases, SARS-CoV-2 spread across the world, causing an unprecedented global pandemic that, by October 2021, incurred over 240 million human cases and more than 4.8 million deaths (https://covid19.who.int/).

Coronaviruses are positive-sense, single-stranded RNA viruses. Although coronaviruses usually cause mild respiratory infection in humans, they can also infect a range of other species, resulting in broad clinical outcomes, varying from subclinical or mild-to-severe respiratory to gastroenteric infections, which, in some cases, can lead to fatal disease (2). Historically, several zoonotic coronaviruses have spilled over into humans, including SARS-CoV, which was described in China in 2002, and Middle East respiratory syndrome coronavirus (MERS-CoV), identified in Saudi Arabia in 2012. Interestingly, SARS-CoV, MERS-CoV, and SARS-CoV-2 present remarkable differences in infection

outcomes. The fatality rates of SARS-CoV and MERS-CoV, for example, are much higher (~10% and ~35%, respectively) than that described for SARS-CoV-2 (<3%) (3, 4). The clinical outcomes of SARS-CoV-2 infection are variable, ranging from asymptomatic infections, which represent most cases, to multiple-organ failure and death (5). Importantly, the most severe cases of COVID-19 resulting in death have been associated with other underlying health conditions (6, 7). In addition, age is another risk factor that has been associated with distinct and often more severe outcomes of SARS-CoV-2 infection. While most human infections with SARS-CoV-2 lead to subclinical disease or only mild symptoms in young healthy adults, disease severity and mortality rates increase with age among individuals older than 30 years (8, 9). Additionally, viral load, which is a direct measure of virus replication and has been linked to severe disease outcomes, has also been shown to increase with the age of affected individuals (8, 10). The mechanisms underlying the different SARS-CoV-2 infection outcomes and the contribution of comorbidities or age to these diverse outcomes, however, remain unknown.

The first step of SARS-CoV-2 infection involves binding of the viral spike (S) protein, more precisely the S receptor binding domain (RBD), to angiotensin-converting enzyme 2 (ACE2), the viral cognate receptor (11, 12). Following S RBD-ACE2 binding, the S protein is cleaved by host proteases (e.g., furin) into the S1/S2 subunits. The next step that takes place is cleavage of the S2 subunit at the S2′ site by the transmembrane serine protease 2 (TMPRSS2), which leads to conformational changes that expose the fusion peptide, enabling membrane fusion and completion of viral entry into host cells (12). In humans, ACE2 is expressed in various cells and tissues, with high levels of the protein being expressed in the upper respiratory tract (URT) (13–15). Notably, differential ACE2 and TMPRSS2 expression have been described in young and elderly people, with a higher percentage of ACE2- and TMPRSS2-expressing cells being detected in the nasal brushing of older people compared to young individuals (16, 17).

Here, we assessed the effect of age on SARS-CoV-2 infection in ferrets. We compared the susceptibility of young (6-month-old) and aged (18- to 39-month-old) ferrets to four different doses of SARS-CoV-2. Viral replication, viral load, and shedding in respiratory secretions and feces were monitored by real-time reverse transcriptase PCR (rRT-PCR), virus isolation, and titrations for 14 days postinoculation (pi), while seroconversion was assessed by virus neutralization assays. The virological and serological findings were used to estimate the median infectious dose ($ID_{50}$) of SARS-CoV-2 in young and aged ferrets. Additionally, expression of ACE2 and TMPRSS2 was assessed in URT and lower respiratory tract (LRT) of ferrets and correlated with outcomes of SARS-CoV-2 infection and replication.

## RESULTS

**Intranasal inoculation of SARS-CoV-2 in young and aged ferrets results in subclinical infection.** To assess the susceptibility of ferrets to SARS-CoV-2, a total of 40 (20 young [6-month-old] and 20 aged [18- to 39-month-old]) animals were allocated in 10 experimental groups ($n = 4$ per group). Animals were mock inoculated (control group) or inoculated intranasally with different doses of SARS-CoV-2 ($10^1$, $10^2$, $10^3$, and $10^6$) (Fig. 1A). Virus-inoculated ferrets were housed in the animal biosafety level 3 (ABSL-3) facility at the East Campus Research Facility (ECRF) at Cornell University. Control animals (four young and four aged animals) were kept under ABSL-1 conditions. Both inoculated and control ferrets were housed individually in Horsfall HEPA filter cages throughout the 14-day experimental period. Following inoculation, clinical parameters, including temperature, body weight, activity, and signs of respiratory disease, were monitored daily. The body temperature in both age groups remained within physiological ranges throughout the experimental period, and no differences were observed between experimental groups (Fig. 1B and C). The body weight had slight variation in all groups, but no difference was noticed between SARS-CoV-2-inculated groups and the mock control ferrets (normalized; day 0 represents 100%) in both young and aged animals (Fig. 1D and E). No clinical signs were observed in young and aged ferrets, even when the highest viral dose ($10^6$ PFU) was
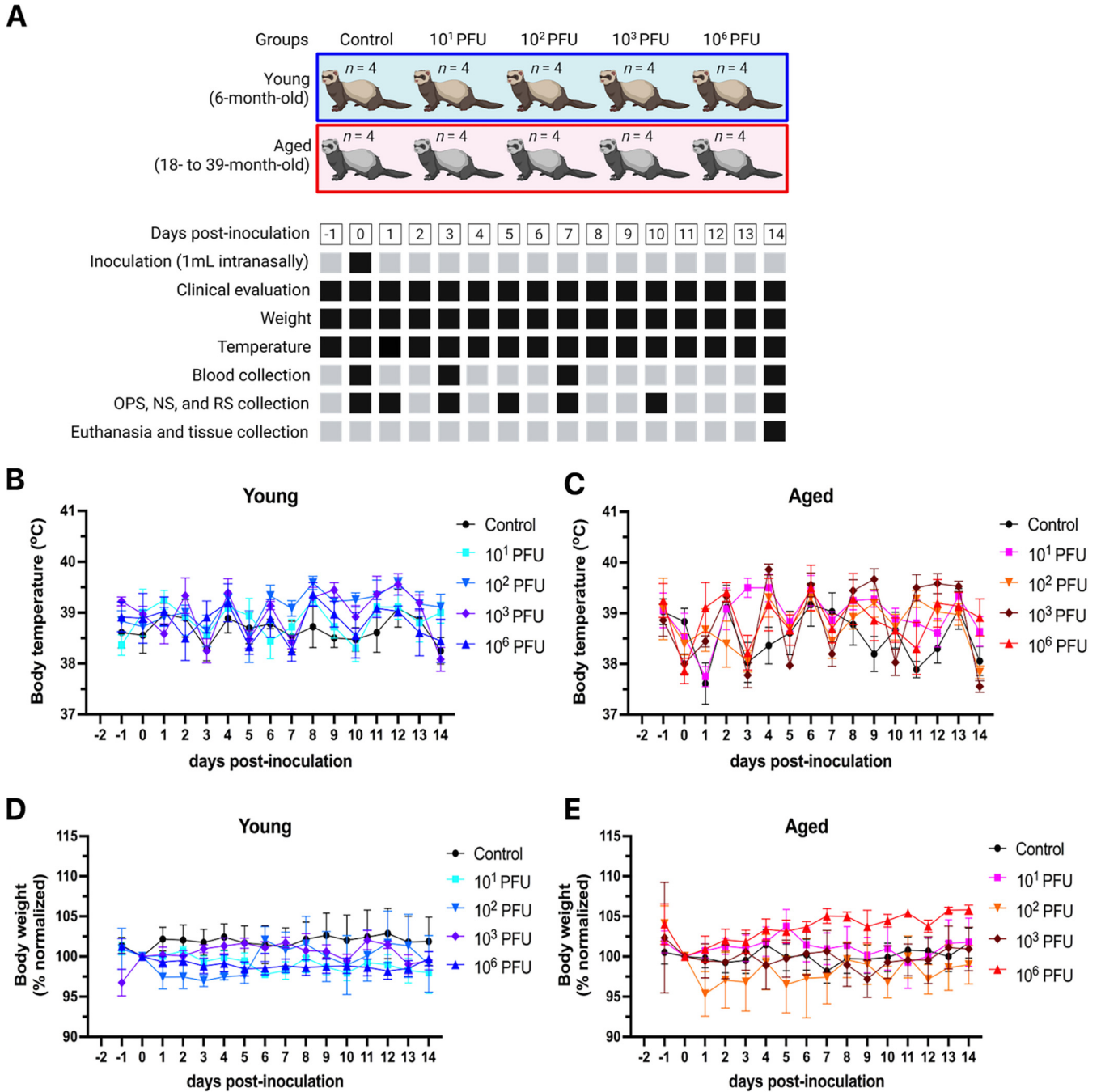
**FIG 1** Experimental design, body weight, and temperature following SARS-CoV-2 inoculation. Forty ferrets (*Mustela putorius furo*), 20 young (6 months old) and 20 aged (18 to 39 months old [30.5 ± 5.3; average ± SD]) were allocated to 10 experimental groups (4 animals per group). Animals were inoculated intranasally with 1 ml (0.5 ml per nostril) MEM (mock control groups) or with a 1-ml virus suspension containing $10^1$, $10^2$, $10^3$, and $10^6$ PFU of SARS-CoV-2 isolate NY67-20 on day 0. All animals were maintained individually in Horsfall HEPA-filtered cages. Clinical parameters, including temperature, body weight, activity, and signs of respiratory disease were monitored daily for 14 days postinoculation (pi). Oropharyngeal (OPS), nasal (NS), and rectal swab (RS) and blood samples were collected at various times postinoculation. Animals were humanely euthanized on day 14 pi. Following necropsy, tissues were collected and processed for rRT-PCR and virus isolation. (A) Black hatched squares represent actual collection/measure time points for each sample type/parameter described. (B and C) Body temperature following intranasal SARS-CoV-2 inoculation recorded throughout the experimental period in young (B) or aged (C) ferrets. (D and E) Body weight measurements throughout the experimental period in young (D) or aged (E) ferrets expressed as percent weight on day 0 (individual ferret weight was normalized to day 0, which represents 100%).

inoculated. No marked differences in daily activity of mock control- or SARS-CoV-2-inoculated animals were noticed. It is important to note that young and aged ferrets naturally exhibit differences in behavior (18). While young animals are more active and curious, aged ferrets are less active and are more restful and calmer than young animals, and this
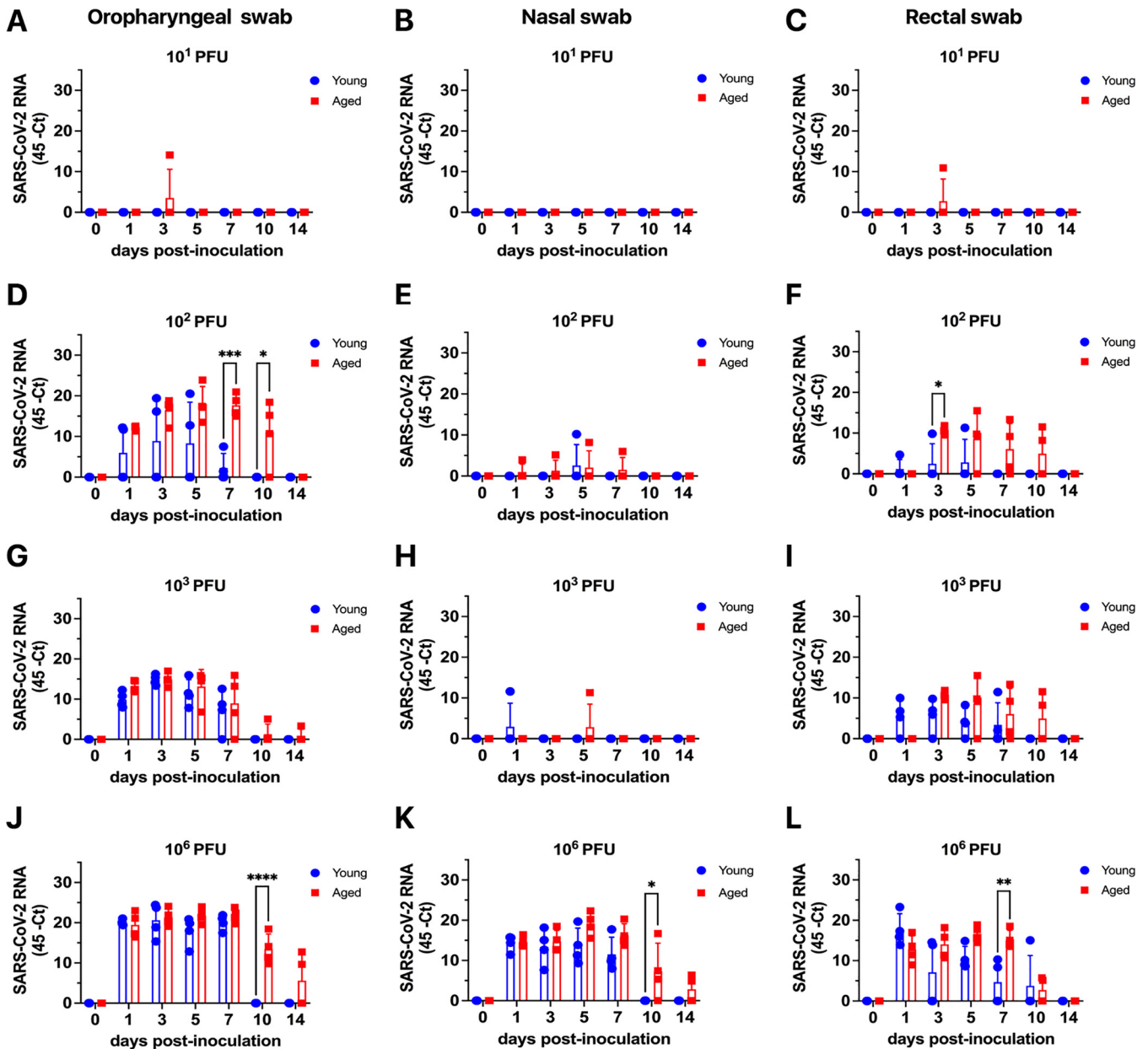
**FIG 2** Viral RNA in respiratory secretion and feces following SARS-CoV-2 inoculation. (A, B, and C) Detection of viral RNA in oropharyngeal (OPS), nasal (NS), and rectal (RS) swab samples in young (6 months) and aged (29 ± 3 months; average ± SD) ferrets inoculated with $10^1$ PFU of SARS-CoV-2. (D, E, and F) Detection of viral RNA in OPS, NS, and RS samples in young and aged ferrets (36 ± 2 months; average ± SD) inoculated with $10^2$ PFU of SARS-CoV-2. (G, H, and I) Detection of viral RNA in OPS, NS, and RS samples in young and aged (30 ± 2 months; average ± SD) ferrets inoculated with $10^3$ PFU of SARS-CoV-2. Detection of viral RNA in OPS, NS, and RS samples (J, K, and L, respectively) in young and aged ferrets (31 ± 3 months; average ± SD) inoculated with $10^6$ PFU of SARS-CoV-2. Viral RNA loads are expressed as 45 rRT-PCR cycles minus the actual $C_T$ value. Day 0 represents swab samples collected prior to inoculation with SARS-CoV-2. ****, $P < 0.0001$; ***, $P < 0.001$; **, $P < 0.002$ *, $P < 0.02$.

was also observed in our study. Additionally, no clinical signs of respiratory disease were observed in any of the SARS-CoV-2-inoculated or control mock-inoculated ferrets throughout the experimental period.

**Aged ferrets shed higher viral loads in respiratory secretions and feces than young ferrets.** The dynamics of SARS-CoV-2 replication and shedding were monitored in respiratory secretions and feces by rRT-PCR following inoculation. Oropharyngeal (OPS), nasal (NS), and rectal (RS) swab samples were collected on days 0, 1, 3, 5, 7, 10, and 14 postinoculation (pi) (Fig. 1A). Viral RNA was detected throughout the experiment in young and aged ferrets in SARS-CoV-2-inoculated animals at various levels until day 14 pi. Higher levels of viral RNA were detected in OPS than NS and RS (Fig. 2). Detection of

viral RNA in animals inoculated with $10^1$ PFU of SARS-CoV-2 was restricted to a single aged ferret on day 3 pi in which viral RNA was detected in OPS and RS samples (Fig. 2A and C). In the groups inoculated with $10^2$ PFU, 2/4 young ferrets tested positive by rRT-PCR on days 1 to 5 pi, while 4/4 aged animals were positive on days 1 to 7 pi. Importantly, viral RNA loads in OPS and RS samples were significantly higher in aged animals on days 3 ($P < 0.02$), 7, and 10 pi ($P < 0.001$ and $P < 0.02$) (Fig. 2D and F). In the groups inoculated with $10^3$ PFU, all young (4/4) and aged (4/4) ferrets tested positive for SARS-CoV-2 RNA in OPS samples between days 1 and 5 pi, and viral RNA loads were similar between young and aged animals (Fig. 2G). Viral RNA was detected in RS samples in 2 to 3 of 4 animals in both young and aged groups until day 10 pi (Fig. 2I). In the groups inoculated with $10^6$ PFU, SARS-CoV-2 RNA was consistently detected in OPS, NS, and RS samples between days 1 and 5 pi in both young and aged animals (Fig. 2J to L). Interestingly, marked differences in SARS-CoV-2 RNA load were observed in NS on day 7 pi ($P < 0.02$) and in OPS and RS samples on day 10 pi ($P < 0.0001$ and $P < 0.002$, respectively) among young and aged ferrets.

To assess shedding of infectious virus in young and aged ferrets inoculated with SARS-CoV-2, rRT-PCR-positive respiratory and fecal samples were subjected to virus isolation in cell culture. Infectious SARS-CoV-2 was isolated from OPS samples from 2/4 young ferrets and from 4/4 aged ferrets inoculated with $10^2$ PFU in at least one time point following infection (Fig. 3A and B). Higher frequency of infectious virus shedding was detected between days 3 and 5 pi (Fig. 3A and B). In the group inoculated with $10^3$ PFU, infectious virus shedding was detected in OPS of all young and aged ferrets (Fig. 3C and D). No infectious virus was detected in NS or RS samples in the groups inoculated with $10^2$ or $10^3$ PFU (Fig. 3A to D). In the group inoculated with $10^6$ PFU, SARS-CoV-2 was isolated in 4/4 young and aged ferrets, with all animals in the aged group shedding infectious virus between days 1 and 7 pi (Fig. 3F). Infectious SARS-CoV-2 was also isolated from NS samples from 2/4 young and 4/4 aged animals (Fig. 3E and F).

In addition to virus isolation, all the OPS samples that tested positive by rRT-PCR were subjected to virus quantitation. Peak viral titers were detected between days 3 and 5 pi (Fig. 4). In general, viral titers and the frequency of animals shedding detectable infectious SARS-CoV-2 were higher in the aged group than in young animals (Fig. 4). In animals inoculated with $10^2$ PFU, statistically significant differences in virus shedding between young and aged ferrets were observed on day 5 pi ($P < 0.002$) (Fig. 4A). While 4/4 aged ferrets shed virus (titers ranging from 1.0 to 2.8 $\log_{10}$ $TCID_{50} \cdot ml^{-1}$ [50% tissue culture infectious dose per milliliter]), only 1/4 young ferrets shed 1.0 $\log_{10} TCID_{50} \cdot ml^{-1}$ (Fig. 4A). In animals inoculated with $10^3$ PFU, 4/4 young and aged animals shed infectious virus (Fig. 3C and D) on day 3 pi. Viral titers were significantly higher in aged ferrets than young animals on day 5 pi ($P < 0.001$) (Fig. 4B). Although differences in viral titers were observed between young and aged ferrets inoculated with $10^2$ and $10^3$ PFU at limited time points, these differences were more evident between the age groups in animals inoculated with the highest SARS-CoV-2 dose ($10^6$ PFU). In these groups, infectious virus was recovered from OPS and NS (Fig. 3E and F). While young ferrets shed between 1.0 and 2.0 $\log_{10} TCID_{50} \cdot ml^{-1}$ in OPS secretions, aged animals shed up to 3.8 $\log_{10} TCID_{50} \cdot ml^{-1}$ of virus (days 3 to 5 pi, $P < 0.0001$; day 7 pi, $P < 0.001$; Fig. 4C). Viral titers were above the limit of quantification (1.0 $\log_{10} TCID_{50} \cdot ml^{-1}$) in 4/4 aged ferrets from day 1 to 7 pi; however, in young animals, viral titers were only detected in 2/4 on days 1 and 3 pi and 1/4 on day 5 pi (Fig. 4C). These results indicate that SARS-CoV-2 replication was more efficient in the upper respiratory tract of aged animals, suggesting that aged ferrets are more susceptible to SARS-CoV-2 infection.

**Viral load in tissues.** Viral RNA load and tissue distribution of SARS-CoV-2 were assessed on day 14 pi. Nasal turbinate, soft palate/tonsil, and left and right lungs (cranial and caudal lobes) were collected and processed by rRT-PCR. SARS-CoV-2 RNA was only detected in nasal turbinate and soft palate/tonsil from young and aged ferrets inoculated with $10^6$ PFU (Fig. 5). Viral RNA was detected with high threshold cycle ($C_T$) values in the nasal turbinate of 3/4 and soft palate/tonsil of 2/4 young ferrets, while in aged animals, the nasal turbinate of 4/4 and the soft palate/tonsil of 3/4 animals were
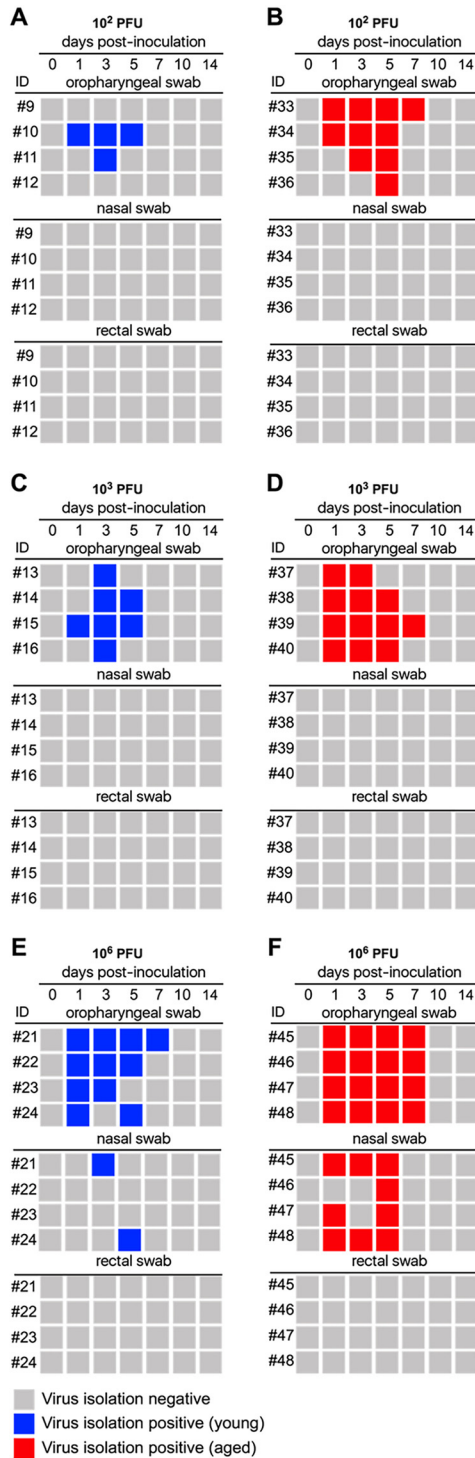
**FIG 3** Shedding of infectious SARS-CoV-2 in respiratory secretions and feces. The rRT-PCR-positive respiratory and fecal samples were subjected to virus isolation in cell culture. (A and B) Detection of infectious virus in oropharyngeal (OPS), nasal (NS), and rectal (RS) swab samples of young (6 months) (A) and aged (36 $\pm$ 2 months; average $\pm$ SD) (B) ferrets inoculated with $10^2$ PFU of SARS-CoV-2. (C and D) Detection of infectious virus in OPS, NS, and RS samples of young (6 months) (C) and aged (30 $\pm$ 2 months; average $\pm$ SD) (D) ferrets inoculated with $10^3$ PFU of SARS-CoV-2. (E and F) Detection of infectious virus in OPS, NS, and RS samples of young (6 months) (E) and aged (31 $\pm$ 3 months; average $\pm$ SD) (F) ferrets inoculated with $10^6$ PFU of SARS-CoV-2. At least three blind passages were conducted with each sample. Isolation of SARS-CoV-2 was confirmed by immunofluorescence assay using SARS-CoV-2-specific antibodies. Day 0 represents swab samples collected prior to inoculation with SARS-CoV-2.
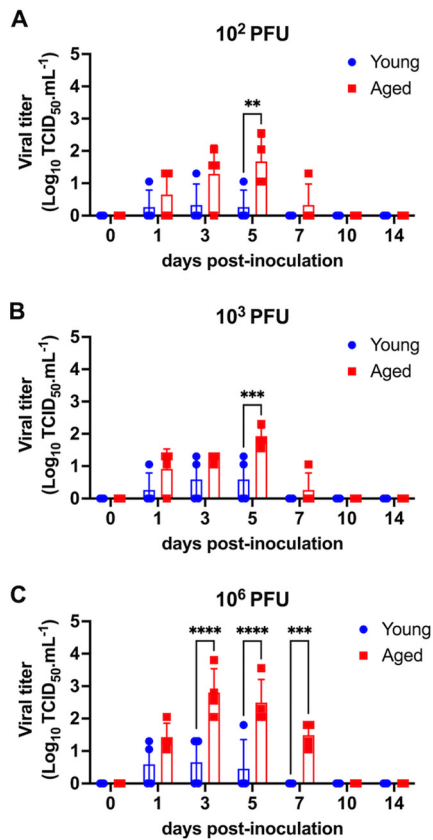
**FIG 4** Infectious SARS-CoV-2 loads in oropharyngeal secretion. Oropharyngeal swab samples (OPS) that tested positive by rRT-PCR were subjected to virus quantitation. Viral titers in young (6 months) and aged (18 to 39 months [30.5 $\pm$ 5.3; average $\pm$ SD]) ferrets inoculated with $10^2$ PFU (A), $10^3$ PFU (B), or $10^6$ PFU (C) of SARS-CoV-2. Virus titers were determined using endpoint dilutions and the Spearman and Karber's method and expressed as $\log_{10}$ TCID$_{50}$·ml$^{-1}$. Day 0 represents swab samples collected prior to inoculation with SARS-CoV-2. ****, $P < 0.0001$; ***, $P < 0.001$; **, $P < 0.002$ *, $P < 0.02$.

rRT-PCR positive. While the tissues were positive for viral RNA, no infectious virus was recovered after three blind passages in cell culture.

**Neutralizing antibody responses to SARS-CoV-2.** The serological response to SARS-CoV-2 was assessed by virus neutralization (VN) assay. All control (mock-inoculated) animals and those inoculated with $10^1$ PFU remained seronegative until the end of the experiment on day 14 pi (Fig. 6A). In the groups inoculated with $10^2$ PFU of SARS-CoV-2, 2/4 young and 4/4 aged ferrets seroconverted and presented neutralizing antibody titers on day 14 pi (Fig. 6B) ($P < 0.02$). All animals in the $10^3$ PFU group, regardless of age, seroconverted by day 14 pi, and no differences in NA titers between age groups were detected (Fig. 6C). Among the animals inoculated with the highest dose ($10^6$ PFU), both young and aged ferrets seroconverted as early as day 7 pi, with higher antibody titers being detected on day 14 pi (Fig. 6D). Together, these results confirm successful infection of 2/4 young ferrets and 4/4 aged ferrets inoculated with $10^2$ PFU of SARS-CoV-2.

**Aged ferrets are more likely to get infected when exposed to lower infectious dose of SARS-CoV-2 than young animals.** The infectivity of SARS-CoV-2 in young and aged ferrets was assessed using three parameters: (i) rRT-PCR in oropharyngeal secretion, (ii) virus isolation in oropharyngeal secretion, and (iii) seroconversion to SARS-CoV-2 on day 14 pi. This resulted in three binary (i.e., positive or negative) response variables for each ferret in the study. Each animal was determined to be infected when at least two of the three parameters evaluated were positive. It is important to note that rRT-PCR results alone were not used as a definitive proof of infection; shedding of infectious virus or seroconversion was also required to define an animal as infected.
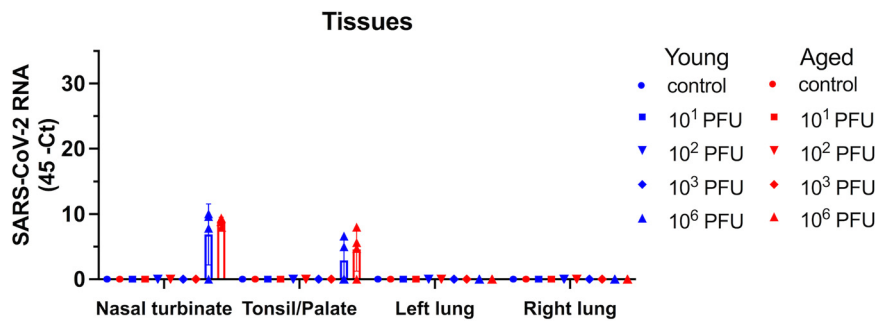
**FIG 5** Viral RNA in tissues following SARS-CoV-2 inoculation. Viral RNA load and tissue distribution of SARS-CoV-2 were assessed on day 14 postinoculation (pi) in nasal turbinate, soft palate/tonsil, and left and right lungs (cranial and caudal lobes). Results of rRT-PCR for all 10 groups doses, including young (6 months) and age (18 to 39 months [30.5 ± 5.3; average ± SD]) ferrets, are shown.

Notably, all three parameters (rRT-PCR-positive OPS, virus isolation [VI]-positive OPS, and seroconversion) used to determine the infection status of young and aged ferrets provided consistent outcomes (Table 1). None of the animals in the young or aged groups shed infectious virus or seroconverted when inoculated with $10^1$ PFU of SARS-CoV-2, indicating no infection. In animals inoculated with $10^2$ PFU, 2/4 young animals tested positive by rRT-PCR and virus isolation and the same two animals seroconverted, as determined by detection of NA on day 14 pi, while all aged ferrets inoculated with $10^2$ PFU were rRT-PCR and virus isolation positive and seroconverted to SARS-CoV-2. All young and aged animals inoculated with $10^3$ and $10^6$ PFU tested positive by rRT-PCR and infectious virus and seroconverted to SARS-CoV-2 by day 14 pi. Based on the infection status of the animals, the estimated median infectious dose ($ID_{50}$) for SARS-CoV-2 in aged ferrets was 31.6 PFU (~32), while in young animals the $ID_{50}$ was estimated at 100.1 PFU (~100; Fig. 7).

**Higher levels of ACE2 and TMPRSS2 transcription in the respiratory tract of aged ferrets compared to young animals.** To investigate factors that could contribute to susceptibility of young and aged ferrets to SARS-CoV-2, we assessed transcription of ACE2 and TMPRSS2, two critical viral entry factors, in the upper (nasal turbinates) and lower (lungs) respiratory tracts of all animals in the study (young [$n = 20$] and aged ferrets [$n = 20$]) by qRT-PCR. Notably, ACE2 and TMPRSS2 mRNA levels were higher in the nasal turbinates of aged ferrets than in young animals ($P < 0.05$) (Fig. 8A and B). No differences in transcription of ACE2 and TMPRSS2 between age groups were observed in the lungs (Fig. 8C and D). Additionally, transcription of ACE2 was higher in the URT than the LRT in both young and aged animals ($P < 0.05$ and $P < 0.0001$, respectively) (Fig. 8E and G). Transcription levels of TMPRSS2, on the other hand, were higher in the LRT than URT in both young and aged ferrets ($P < 0.0001$) (Fig. 8F and H).

## DISCUSSION

Here, we compared the susceptibility of young and aged ferrets to SARS-CoV-2 and assessed the infectivity of the virus by inoculating young and aged animals with increasing viral doses. As evidenced by SARS-CoV-2 replication in the upper respiratory tract, virus shedding in respiratory secretions (viral RNA and infectious virus), and seroconversion following intranasal inoculation, our study shows that aged ferrets are more susceptible than young ferrets to SARS-CoV-2 infection.

Intranasal inoculation of $10^1$ PFU of SARS-CoV-2 did not result in productive infection in young or in aged ferrets. While all aged animals were successfully infected after inoculation with $10^2$ PFU/animal, only 2 of 4 young ferrets were infected with this viral dose. Importantly, the infection rates observed in young and aged animals were consistent and supported by all three criteria used to define productive infection: (i) positive rRT-PCR, (ii) infectious virus shedding in respiratory secretions, and (iii) seroconversion (Table 1). These results suggest that the infectious dose of SARS-CoV-2 required to infect aged ferrets is lower than the dose required to infect young animals. Indeed, the $ID_{50}$ estimated using the three-parameter logistic dose-response model in aged animals was ~32 PFU, while in young animals it was ~100
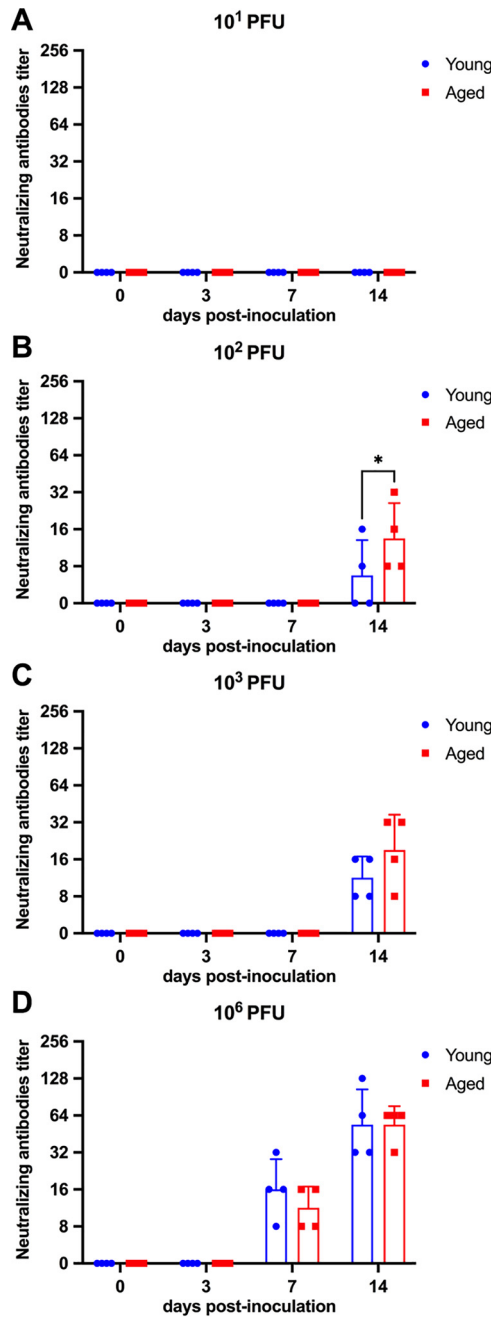
**FIG 6** Neutralizing antibody responses to SARS-CoV-2. Serological response to SARS-CoV-2 was assessed by virus neutralization assay. Serum samples were collected on days 0, 3, 7, and 14 postinoculation (pi). (A to D) Neutralizing antibody responses in young (6 months) and aged (18 to 39 months [30.5 $\pm$ 5.3; average $\pm$ SD]) ferrets inoculated with $10^1$ (A), $10^2$ (B), $10^3$ (C), and $10^6$ PFU (D) of SARS-CoV-2. Neutralizing antibody titers represent the reciprocal of the highest dilution of serum that completely inhibited SARS-CoV-2 infection/replication. Day 0 represents serum samples collected prior to inoculation with SARS-CoV-2. The starting dilution/cutoff VN titer was 8. Neutralizing antibody titers are expressed as the reciprocal of serum dilutions presenting 100% neutralization of 200 $TCID_{50}$ of actual SARS-CoV-2 virus. *, $P < 0.02$.

PFU ($\sim 3\times$ higher). Similarly, a recent study conducted with a French SARS-CoV-2 isolate (UCN19) demonstrated successful infection of 10-month-old ferrets with $2 \times 10^3$ PFU of the virus (19). Interestingly, when younger ferrets (7 months old) and a lower dose ($5 \times 10^2$ PFU per animal) were used, only 1 of 6 inoculated ferrets was infected after intranasal inoculation with a SARS-CoV-2 isolate from Australia (Victoria/1/2020) (20). Despite inherent experimental differences, observations from these earlier studies are consistent with the results presented

**TABLE 1** Median infectious dose data

| Dose (PFU) | Young | | | Aged | | |
| --- | --- | --- | --- | --- | --- | --- |
| | rRT-PCR | Virus isolation | Serology | rRT-PCR | Virus isolation | Serology |
| Control | 0/4 (0%) | 0/4 (0%) | 0/4 (0%) | 0/4 (0%) | 0/4 (0%) | 0/4 (0%) |
| $10^1$ | 0/4 (0%) | 0/4 (0%) | 0/4 (0%) | 1/4 (25%) | 0/4 (0%) | 0/4 (0%) |
| $10^2$ | 2/4 (50%) | 2/4 (50%) | 2/4 (50%) | 4/4 (100%) | 4/4 (100%) | 4/4 (100%) |
| $10^3$ | 4/4 (100%) | 4/4 (100%) | 4/4 (100%) | 4/4 (100%) | 4/4 (100%) | 4/4 (100%) |
| $10^6$ | 4/4 (100%) | 4/4 (100%) | 4/4 (100%) | 4/4 (100%) | 4/4 (100%) | 4/4 (100%) |

here demonstrating a higher susceptibility of older ferrets to SARS-CoV-2. It is important to note, however, that both UCN19 and Victoria/1/2020 isolates belong to early SARS-CoV-2 lineages (lineage A) that do not contain the spike mutation D614G, which is present in the isolate NYI67-20 (lineage B.1) used in our study. This is relevant, as several studies have shown that the S D614G mutation is associated with increased infectivity and transmission of SARS-CoV-2 in animal models and in humans (21–25).

Differences in viral RNA load between age groups inoculated with the same viral doses were observed mainly on days 7 and 10 pi, when aged ferrets remained positive, while viral RNA was no longer detected in most young animals. The highest viral loads were detected on OPS samples compared to NS and RS. Higher viral loads in OPS or nasopharyngeal swab (NPS) samples have also been described in humans compared to sputum or anterior nares samples (ANS) (26–29). Most importantly, shedding of infectious virus in aged ferrets inoculated with SARS-CoV-2 was prolonged compared to that in young animals, and the viral titers detected in this age group were higher than those detected in young animals.

Infectious virus was isolated from aged ferrets with a higher frequency and for prolonged time compared to young animals. These differences were more pronounced in animals inoculated with the highest viral dose ($10^6$ PFU), from which infectious virus was isolated from all four aged ferrets from day 1 to 7 pi. Additionally, the viral titers were significantly higher in aged animals than young ferrets on day 5 pi in the $10^2$ PFU ($P < 0.002$) and $10^3$ PFU ($P < 0.001$) groups and on days 3, 5, and 7 pi in the $10^6$ PFU group ($P < 0.001$). Together, these results demonstrate that SARS-CoV-2 replicates more efficiently in aged ferrets than young animals. Regardless of the viral dose, after day 7 pi, no infectious virus was isolated from any animal inoculated with the different
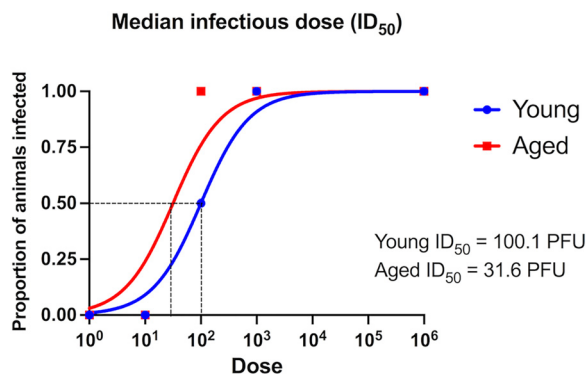


**Median infectious dose (ID$_{50}$)**

Young ID$_{50}$ = 100.1 PFU
Aged ID$_{50}$ = 31.6 PFU

**FIG 7** Estimated ID$_{50}$ of SARS-CoV-2 in young (6 months) and aged (18 to 39 months [30.5 $\pm$ 5.3; average $\pm$ SD]) ferrets. The infectivity of SARS-CoV-2 in young and aged ferrets was assessed by using three parameters: (i) rRT-PCR in oropharyngeal secretion, (ii) virus isolation in oropharyngeal secretion, and (iii) seroconversion to SARS-CoV-2 on day 14 postinoculation. For rRT-PCR and virus isolation, an animal was considered positive if it tested positive at any time point throughout the 14-day experimental period. Each ferret was determined to be infected when at least two of the three parameters evaluated were positive. Median infectious dose (ID$_{50}$) of SARS-CoV-2 was estimate using the three-parameter logistic dose-response model.
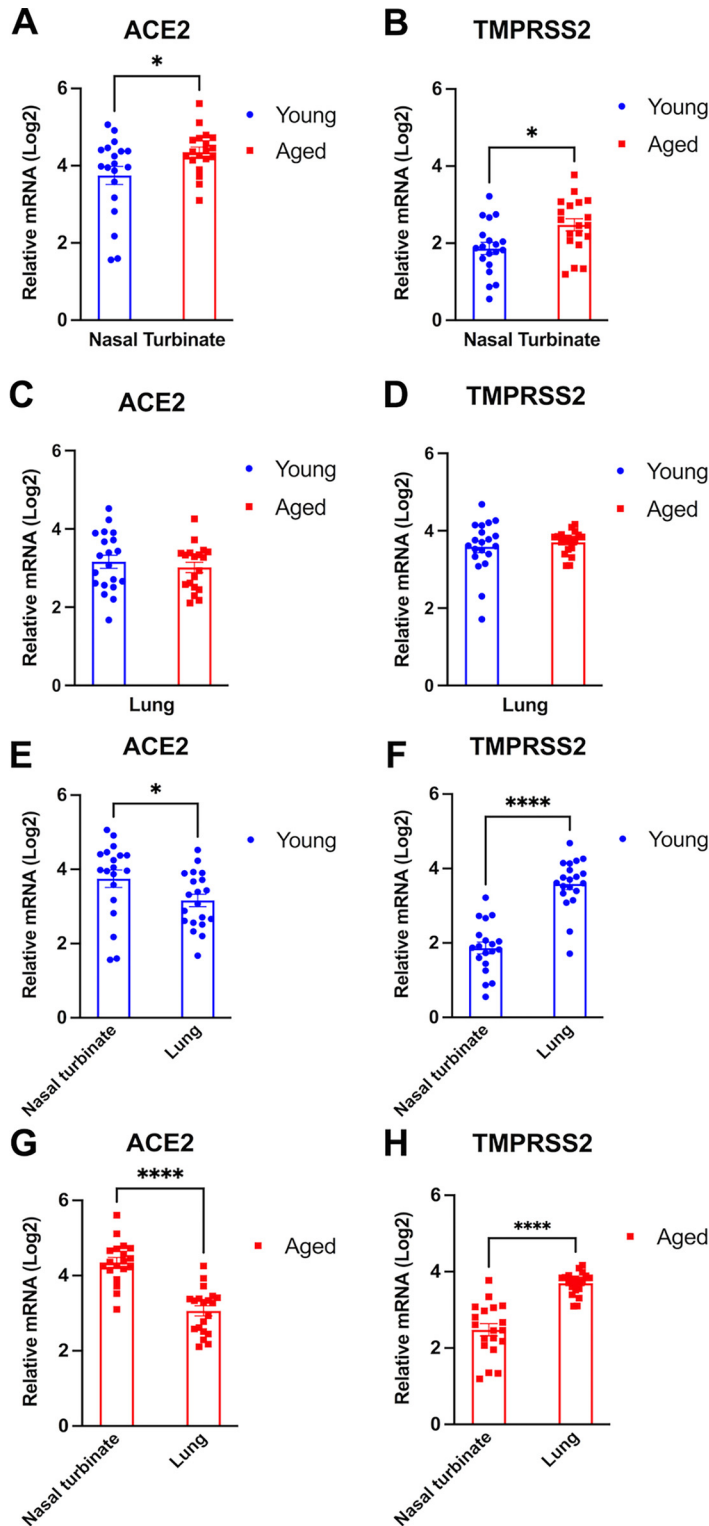
**FIG 8** Expression of ACE2 and TMPRSS2 in the respiratory tract of young and aged ferrets. The levels of ACE2 and TMPRSS2 expression in the upper (nasal turbinates) and lower (lungs) respiratory tracts of all ferrets in the study were assessed by qRT-PCR. Expression levels of ACE2 and TMPRSS2 (A and B, respectively) in nasal turbinates of young (6 months) and aged (18 to 39 months [30.5 $\pm$ 5.3; average $\pm$ SD]) ferrets are shown. Expression levels of ACE2 and TMPRSS2 (C and D, respectively) in the lungs of young and aged ferrets are shown. Expression levels of ACE2 and TMPRSS2 in nasal turbinates and lung of young (E and F, respectively) and aged (G and H, respectively) ferrets are shown. ****, $P < 0.0001$; ***, $P < 0.001$*, $P < 0.05$.
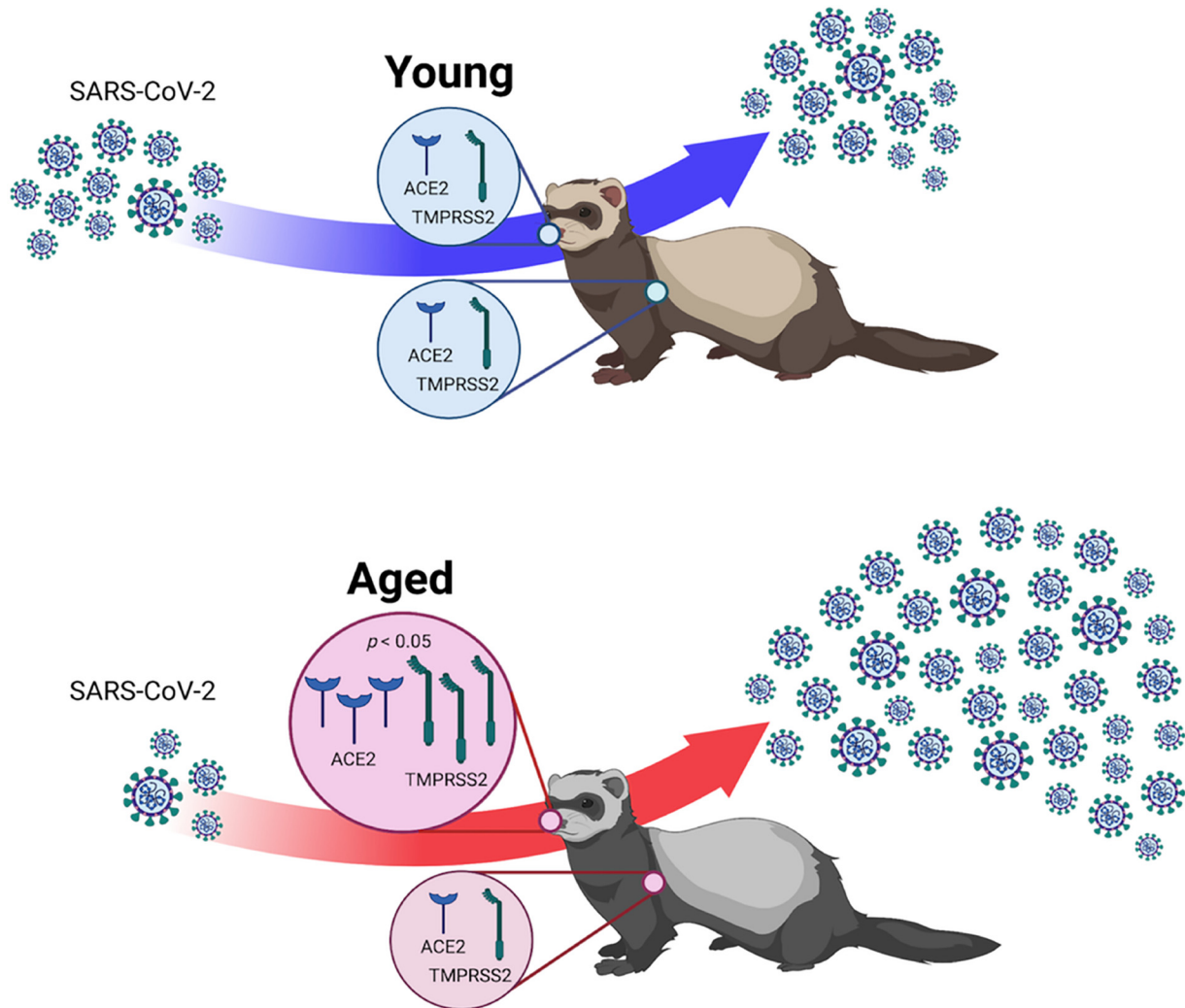
**FIG 9** Age-related differential susceptibility to SARS-CoV-2 infection. Aged ferrets were more likely to get infected when exposed to lower infectious doses of the virus than young animals. SARS-CoV-2 replication in the upper respiratory tract and shedding in respiratory secretions is enhanced in aged ferrets compared to young animals. Notably, aged ferrets express higher levels of ACE2 and TMPRSS2 in the upper respiratory tract. Together these results suggest that the higher infectivity and enhanced ability of SARS-CoV-2 to replicate in aged individuals is associated with expression levels of two of the molecules that are critical for SARS-CoV-2 infection and host cell entry.

viral doses, despite detection of viral RNA by rRT-PCR up to day 10 to 14 pi. These results corroborate virus shedding patterns observed in humans in which the infectious period was shown to last 7 to 10 days following onset of clinical signs (30). Importantly, in humans a decrease in SARS-CoV-2 infectivity parallels increased levels of neutralizing antibodies in serum (4, 30). This was also observed here, which suggests that antibody responses play a role in viral clearance. Innate immune responses at the site of virus replication, however, may also play a role and contribute to control the infection in the respiratory tract.

Our findings showing higher susceptibility of aged ferrets to SARS-CoV-2 infection in the present study parallel clinical observations in humans, which point to increased susceptibility and higher levels of virus replication in the respiratory tract of older people compared to young children (8, 10). Additionally, results presented here corroborate findings of a recent study by Kim and collaborators (31), who showed age-related differences in viral load in the respiratory tract and lung histopathology in ferrets inoculated with SARS-CoV-2. This study also showed that expression levels of genes related to the interferon (IFN) pathway, activated T cells, and macrophage responses were increased in older ferrets following SARS-CoV-2 infection (31). These changes are

likely due to enhanced immune responses following higher viral replication in aged animals. Based on our $ID_{50}$ estimates indicating that the infectious dose of SARS-CoV-2 is $\sim 3\times$ higher in young ferrets ($\sim$100 PFU) than aged animals ($\sim$32 PFU), we hypothesized that differential expression of key SARS-CoV-2 entry factors, such as the ACE2 receptor and the TMPRSS2 protease, could underlie age-related differences in their susceptibility to SARS-CoV-2. Notably, we showed that transcription of both ACE2 and TMPRSS2 were lower in nasal turbinates (primary site of SARS-CoV-2 replication in the URT) of young ferrets compared to mRNA levels in aged animals. Additionally, transcription of ACE2 was higher in the URT than the lung (LRT). These observations corroborate findings in humans (16) and suggest that differences in ACE2 and TMPRSS2 mRNA levels in the respiratory tract contribute to age-related susceptibility to SARS-CoV-2. In future studies it will be important to investigate expression of ACE2 and TMPRSS2 proteins in URT and determine the dynamic changes in their expression throughout the course of SARS-CoV-2 infection in young and aged ferrets. The spectrum of factors that can contribute to SARS-CoV-2 susceptibility, however, is broad, and further studies are needed to assess the function and involvement of other entry and immune response-related factors on SARS-CoV-2 infection and replication in different age groups. The young and aged ferret models developed here provide an excellent platform to investigate age-related differences in susceptibility to SARS-CoV-2 infection and replication and the host and viral factors that play a role in these dynamic interactions. This model may be particularly useful to dissect the mechanisms/functions emerging in several of the SARS-CoV-2 variants (e.g., P.1 and B.1.617.2), which seem to have an enhanced ability to infect younger individuals.

In summary, here we demonstrated that age affects susceptibility of ferrets to SARS-CoV-2, with aged animals being more likely to get infected when exposed to lower infectious doses of the virus than young animals. Additionally, SARS-CoV-2 replication in the URT and shedding in respiratory secretions is enhanced in aged ferrets compared to young animals. We also showed that, similar to what has been described in humans (16), aged ferrets present higher levels of ACE2 and TMPRSS2 mRNAs, two key factors determining virus entry into cells, in the URT (Fig. 9). Together, these results suggest that the higher infectivity and enhanced ability of SARS-CoV-2 to replicate in aged individuals is associated, at least in part, with transcription/expression levels of ACE2 and TMPRSS2 at the sites of virus entry.

## MATERIALS AND METHODS

**Virus and cells.** Vero E6 (ATCC CRL-1586) and Vero E6/TMPRSS2 (JCRB1819; JCRB Cell Bank) cells were cultured in Dulbecco's modified Eagle medium (DMEM) supplemented with 10% fetal bovine serum (FBS), L-glutamine (2 mM), penicillin (100 U·ml$^{-1}$), streptomycin (100 $\mu$g·ml$^{-1}$), and gentamicin (50 $\mu$g·ml$^{-1}$). The cell cultures were maintained at 37°C with 5% $CO_2$. The SARS-CoV-2 isolate NYI67-20 (B.1 lineage) was propagated in Vero E6 cells. Low-passage-number virus stocks (passage 3) were prepared, cleared by centrifugation (2,000 $\times$ $g$ for 15 min), and stored at $-$80°C. The whole-genome sequence of the virus stock was determined to confirm that no mutations occurred during passages in cell culture. The titer of virus stock was determined according to the Spearman and Karber method and expressed as PFU per milliliter.

**Animal housing and experimental design.** All animals were handled in accordance with the Animal Welfare Act, and the study procedures were reviewed and approved by the Institutional Animal Care and Use Committee at Cornell University (IACUC approval number 2020-0064). A total of 40 ferrets (*Mustela putorius furo*) were obtained from a commercial breeder (Triple F Farms, Gillett, PA, USA). Twenty young (6-month-old ferrets) and 20 aged (18 to 39 months [30.5 ± 5.3; average ± standard deviation, or SD]) ferrets were randomly allocated to experimental groups ($n = 4$). The age and sex of the ferrets allocated in each group are presented in Table 2. While the control animals were housed at the ASBL-1 facility, all the virus-inoculated ferrets were housed in the ASBL-3 facility at the East Campus Research Facility (ECRF) at Cornell University. After 72 h of acclimation, ferrets were sedated and inoculated intranasally with 1 ml (0.5 ml per nostril) of a virus suspension containing $10^1$, $10^2$, $10^3$, or $10^6$ PFU of SARS-CoV-2 isolate NYI67-20 (groups 2, 3, 4 and 5, respectively [$n = 4$/group]). Ferrets of each age maintained as mock-inoculated control (group 1, $n = 4$) were mock inoculated with Vero E6 cell culture medium supernatant. All ferrets were maintained individually in Horsfall HEPA-filtered cages, connected to the ASBL-3 facility's exhaust system. Body temperatures and weight were measured on a daily basis. Oropharyngeal (OPS), nasal (NS), and rectal (RS) swabs were collected under sedation (dexmedetomidine) on days 0, 1, 3, 5, 7, 10, and 14 pi. Upon collection, swabs were placed in sterile tubes containing 1 ml of viral transport medium (VTM; Corning, Glendale, AZ, USA) and stored at $-$80°C until being processed for further

**TABLE 2** Sex and age of ferrets among the experimental groups[a]

| | Young | | Aged | |
|---|---|---|---|---|
| Dose (PFU) | Sex | Age (mo [avg ± SD]) | Sex | Age (mo [avg ± SD]) |
| Control | 2 F; 2 M | 6 | 3 F; 1 M | 23 ± 6 |
| $10^1$ | 2 F; 2 M | 6 | 4 F | 29 ± 3 |
| $10^2$ | 2 F; 2 M | 6 | 4 F | 36 ± 2 |
| $10^3$ | 2 F; 2 M | 6 | 4 F | 30 ± 2 |
| $10^6$ | 2 F; 2 M | 6 | 3 F; 1 M | 31 ± 3 |

[a]F, female; M, male.

analyses. Blood was collected under sedation (dexmedetomidine) through cranial vena cava venipuncture using a 3-ml sterile syringe and 23-gauge, 1-inch needle and transferred into serum separator tubes on days 0, 3, 7, and 14 pi. The blood tubes were centrifuged at 1,500 × $g$ for 10 min, and serum was aliquoted and stored at −20°C until further analysis. Ferrets were humanely euthanized on day 14 pi under deep inhalatory anesthesia using isoflurane followed by cardiac puncture. Following necropsy, tissues, including nasal turbinate, soft palate/tonsil, and left and right lung, were collected and processed for rRT-PCR and virus isolation.

**Nucleic acid isolation and real-time reverse transcriptase PCR.** Nucleic acid was extracted from OPS, NS, RS, and tissue samples collected at necropsy. For OPS, NS, and RS samples, 200 $\mu$l of cleared swab supernatant was used for nucleic acid extraction. For tissues, 0.2 g of each tissue was minced with a sterile scalpel, resuspended in 2 ml DMEM (10%, wt/vol), and homogenized using a stomacher (one speed cycle of 60 s; Stomacher 80 Biomaster). Next, 200 $\mu$l of the tissue homogenate supernatant was used for RNA extraction using the MagMax Core extraction kit (Thermo Fisher, Waltham, MA, USA) and the automated KingFisher Flex nucleic acid extractor (Thermo Fisher, Waltham, MA, USA) following the manufacturer's recommendations. The real-time reverse transcriptase PCR (rRT-PCR) was performed using the EZ-SARS-CoV-2 real-time RT-PCR assay (Tetracore Inc., Rockville, MD, USA), which detects both genomic and subgenomic viral RNA targeting the virus nucleocapsid protein (N) gene. The limit of detection (LOD) for this assay was previously established as 250 viral genome copies per ml or 1.75 viral genome copies per reaction (32). At this viral concentration, the assay results in mean $C_T$ values of 35.17 in 20 replicates. Based on this LOD, a $C_T$ cutoff of 37.09 was established (35.17 + 3 SD), and all samples with initial $C_T$ values above the cutoff are retested. Only samples with reproducible detection upon repeated testing were considered positive. Viral RNA loads are expressed as 45 rRT-PCR cycles minus the actual $C_T$ value. An internal inhibition control was included in all reactions. Positive and negative amplification controls were run side by side with test samples.

**Virus isolation and titrations.** All OPS, NS, and RS and tissue samples that tested positive for SARS-CoV-2 by rRT-PCR were subjected to virus isolation under BSL-3 conditions. Twenty-four-well plates were seeded with ~75,000 Vero E6/TMPRSS2 cells per well 24 h prior to sample inoculation. Cells were rinsed with phosphate-buffered saline (PBS) (Corning, Glendale, AZ, USA) and inoculated with 150 $\mu$l of each sample, and the inoculum was adsorbed for 1 h at 37°C with 5% $CO_2$. Mock-inoculated cells were used as negative controls. After adsorption, replacement cell culture medium supplemented with FBS as described above was added, and cells were incubated at 37°C with 5% $CO_2$ and monitored daily for cytopathic effect (CPE) for 3 days. SARS-CoV-2 replication in CPE-positive cultures was confirmed with an immunofluorescence assay (IFA) as previously described (33, 34). Cell cultures with no CPE were frozen, thawed, and subjected to two additional blind passages/inoculations in Vero E6/TMPRSS2 cell cultures. At the end of the third passage, the cell cultures were subjected to IFA (33, 34). OPS were subjected to endpoint titrations. For this, the original sample was subjected to limiting dilutions and inoculated into Vero E6/TMPRSS2 cell cultures in 96-well plates. At 48 h postinoculation, cells were fixed with 3.7% formaldehyde for 30 min at room temperature, permeabilized with 0.2% Triton X-100 for 10 min at room temperature (in phosphate buffered saline [PBS]), and subjected to an IFA using a rabbit polyclonal antibody (pAb) specific for the SARS-CoV-2 nucleoprotein (N) (produced in D. G. Diel's laboratory), followed by incubation with goat anti-rabbit IgG (goat anti-rabbit IgG; DyLight 594 conjugate; Immunoreagent Inc.). Virus titers were determined at each time point using endpoint dilutions and the Spearman and Karber's method and expressed as $TCID_{50} \cdot ml^{-1}$.

**Serology.** Neutralizing antibody responses to SARS-CoV-2 were assessed by VN assay performed under BSL-3 laboratory conditions. Twofold serial dilutions (1:8 to 1:1,024) of serum samples were incubated with 100 to 200 $TCID_{50}$ of SARS-CoV-2 isolate NYI67-20 for 1 h at 37°C. Following incubation of serum and virus, 50 $\mu$l of a cell suspension of Vero E6 cells was added to each well of a 96-well plate and incubated for 48 h at 37°C with 5% $CO_2$. The cells were fixed, permeabilized, and subjected to IFA as described above. Unbound antibodies were washed from cell cultures by rinsing the cells PBS, and virus infectivity was assessed under a fluorescence microscope. Neutralizing antibody titers were expressed as the reciprocal of the highest dilution of serum that completely inhibited SARS-CoV-2 infection/replication. FBS and positive and negative serum samples from white-tailed deer fawns (33) were used as controls.

**Expression level of ACE2 and TMPRSS2 genes in the respiratory tract.** RNA samples extracted from nasal turbinate and lungs (described above) were treated with DNA-free kit DNase treatment and removal (Invitrogen, Carlsbad, CA, USA) according to the manufacturer's instructions. The amount of RNA in each sample was measured using a Qubit RNA BR assay kit (Invitrogen, Carlsbad, CA, USA), and then all the samples were diluted in double-distilled water (ddH_2O) to obtain a concentration of 5 ng/$\mu$l.

Standard curves were prepared from a pool of RNA of all samples (2-fold dilutions). Custom primers and probe were designed to angiotensin-converting enzyme 2 (ACE2), transmembrane serine protease 2 (TMPRSS2), and glyceraldehyde 3-phosphate dehydrogenase (GAPDH) of ferrets using PrimerQuest Tool from the Integrated DNA Technologies website (https://www.idtdna.com/pages). The primer and probe sequences for ferret ACE2 were 5'-GATGTGAGGGTGAGCGATTT-3', 5'-GGGACTTCCTGATAGCTTCTTC-3', and 5'-6-FAM/TGACATCAT/ZEN/TCCCAGAGCTGACGT-3'IABkFQ based on *Mustela putorius furo* ACE2, GenBank accession number NM_001310190.1; for ferret, TMPRSS2 sequences were 5'-CGGTGTTTACGGACTGGATTTA-3', 5'-GGTGCCCAGAGAATGAAGAA-3', and 5'-6-FAM/ACAGCTAAT/ZEN/CCATGTGCCCTGTGT-3'-IABkFQ based on *Mustela putorius furo* serine transmembrane protease 2 (TMPRSS2), GenBank accession number NM_001386127.1; and for ferret, GAPDH sequences were 5'-GATGCTGGTGCTGAGTATGT-3', 5'-CAGAAGGAGCAG AGATGATGAC-3', and 5'-6-FAM/TTCACCACC/ZEN/ATGGAGAAGGCTGG-3'-IABkFQ/based on *Mustela putorius furo* GAPDH, GenBank accession number NM_001310173.1. Real-time RT-PCR amplifications were performed in 10-$\mu$l reaction mixtures, with 3 $\mu$l of RNA, 5 $\mu$l of TaqMan RT-PCR mix (TaqMan RNA-to-Ct 1-step kit) (Applied Biosystems, Waltham, MA, USA), 0.5 $\mu$l of TaqMan RT-enzyme mix, 0.25 $\mu$l of the mixture of primers and probe (PrimeTime qPCR probe assays) (Integrated DNA Technologies Inc., Coralville, IA, USA), and 1.25 $\mu$l of ddH$_2$O. Amplification and detection were performed under the following conditions: 15 min at 48℃ for reverse transcription, 10 min at 95℃ for polymerase activation, 40 cycles of 15 s at 95℃ for denaturation, and 1 min at 60℃ for annealing and extension. The measurement of gene expression was performed by using the relative quantitation method (35). Relative genome copy numbers were calculated based on the standard curve determined for each gene within CFX Maestro software (Bio-Rad, Hercules, CA, USA), and expression levels of the genes tested were normalized to the housekeeping gene GAPDH. The amount of relative mRNA detected in each sample was expressed as log$_2$ genome copy number.

**Median infectious dose calculations.** Median infectious dose (ID$_{50}$) of SARS-CoV-2 in young and aged ferrets was assessed by using three parameters: (i) rRT-PCR in oropharyngeal secretion, (ii) virus isolation in oropharyngeal secretion, and (iii) seroconversion to SARS-CoV-2 on day 14 pi. This resulted in three binary (i.e., positive or negative) response variables for each ferret in the study. The frequency (%) of animals positive for each dose inoculated in both young and aged group was determined (Table 1). For rRT-PCR and virus isolation, an animal was considered positive if it tested positive at any time point throughout the 14-day experimental period. Given the consistency of virus shedding detected in oropharyngeal swabs, the frequency of young and aged ferrets shedding virus in oropharyngeal secretions that seroconverted to SARS-CoV-2 were then used to calculate ID$_{50}$. The three-parameter logistic model (3PL) was used to estimate ID$_{50}$. To determine the dose-response curve using 3PL model, viral dose was log transformed, the bottom response value was constrained to 0, and the top response value was constrained to 1. The three-parameter logistic model was implemented in GraphPad Prism software (version 9.0.1).

**Statistical analysis.** Statistical analysis was performed by 2-way analysis of variance (ANOVA) followed by multiple comparisons and by unpaired *t* test. Statistical analysis and data plotting were performed using the GraphPad Prism software (version 9.0.1).

## REFERENCES

1. Gorbalenya AE, Baker SC, Baric RS, de Groot RJ, Drosten C, Gulyaeva AA, Haagmans BL, Lauber C, Leontovich AM, Neuman BW, Penzar D, Perlman S, Poon LLM, Samborskiy DV, Sidorov IA, Sola I, Ziebuhr J. 2020. The species severe acute respiratory syndrome-related coronavirus: classifying 2019-nCoV and naming it SARS-CoV-2. Nat Microbiol https://doi.org/10.1038/s41564-020-0695-z.

2. Masters PS, Perlman S. 2013. Chapter 28–Coronaviridae. *In* Knipe DM, Howley PM, Cohen JI, Griffin DE, Lamb RA, Martin MA, Racaniello VR, Roizman B (ed), Fields virology, 6th ed. Lippincott Williams & Wilkins, Philadelphia, PA.

3. Chen B, Tian EK, He B, Tian L, Han R, Wang S, Xiang Q, Zhang S, El Arnaout T, Cheng W. 2020. Overview of lethal human coronaviruses. Signal Transduct Target Ther 5:89. https://doi.org/10.1038/s41392-020-0190-2.

4. Cevik M, Tate M, Lloyd O, Maraolo AE, Schafers J, Ho A. 2021. SARS-CoV-2, SARS-CoV, and MERS-CoV viral load dynamics, duration of viral shedding, and infectiousness: a systematic review and meta-analysis. Lancet Microbe 2: e13–e22. https://doi.org/10.1016/S2666-5247(20)30172-5.

5. Wu Z, McGoogan JM. 2020. Characteristics of and important lessons from the coronavirus disease 2019 (COVID-19) outbreak in China. JAMA 323: 1239. https://doi.org/10.1001/jama.2020.2648.

6. Bialek S, Boundy E, Bowen V, Chow N, Cohn A, Dowling N, Ellington S, Gierke R, Hall A, MacNeil J, Patel P, Peacock G, Pilishvili T, Razzaghi H, Reed N, Ritchey M, Sauber-Schatz E. 2020. Severe outcomes among patients with coronavirus disease 2019 (COVID-19)—United States, February 12–March 16, 2020. MMWR Morb Mortal Wkly Rep https://doi.org/10.15585/mmwr.mm6912e2.

7. Nachtigall I, Lenga P, Jóźwiak K, Thürmann P, Meier-Hellmann A, Kuhlen R, Brederlau J, Bauer T, Tebbenjohanns J, Schwegmann K, Hauptmann M, Dengler J. 2020. Clinical course and factors associated with outcomes among 1904 patients hospitalized with COVID-19 in Germany: an observational study. Clin Microbiol Infect https://doi.org/10.1016/j.cmi.2020.08.011.

8. Euser S, Aronson S, Manders I, Van Lelyveld S, Herpers B, Sinnige J, Kalpoe J, Van Gemeren C, Snijders D, Jansen R, Stekhoven SS, Van Houten M, Lede I, Cohen Stuart J, Megelink FS, Kapteijns E, Den BJ, Sanders E, Wagemakers A, Souverein D. 2021. SARS-CoV-2 viral load distribution

reveals that viral loads increase with age: a retrospective cross-sectional cohort study. medRxiv https://doi.org/10.1101/2021.01.15.21249691.

9. O'Driscoll M, Ribeiro Dos Santos G, Wang L, Cummings DAT, Azman AS, Paireau J, Fontanet A, Cauchemez S, Salje H. 2021. Age-specific mortality and immunity patterns of SARS-CoV-2. Nature 590:140–145. https://doi.org/10.1038/s41586-020-2918-0.

10. Magleby R, Westblade LF, Trzebucki A, Simon MS, Rajan M, Park J, Goyal P, Safford MM, Satlin MJ. 2020. Impact of severe acute respiratory syndrome coronavirus 2 viral load on risk of intubation and mortality among hospitalized patients with coronavirus disease 2019. Clin Infect Dis https://doi.org/10.1093/cid/ciaa851.

11. Letko M, Marzi A, Munster V. 2020. Functional assessment of cell entry and receptor usage for SARS-CoV-2 and other lineage B betacoronaviruses. Nat Microbiol 5:562–569. https://doi.org/10.1038/s41564-020-0688-y.

12. Hoffmann M, Kleine-Weber H, Schroeder S, Krüger N, Herrler T, Erichsen S, Schiergens TS, Herrler G, Wu N-H, Nitsche A, Müller MA, Drosten C, Pöhlmann S, Mü MA, Drosten C, Pö S, Krüger N, Herrler T, Erichsen S, Schiergens TS, Herrler G, Wu N-H, Nitsche A, Müller MA, Drosten C, Pöhlmann S. 2020. SARS-CoV-2 cell entry depends on ACE2 and TMPRSS2 and is blocked by a clinically proven protease inhibitor. Cell 181:271–280. https://doi.org/10.1016/j.cell.2020.02.052.

13. Chen M, Shen W, Rowan NR, Kulaga H, Hillel A, Ramanathan M, Lane AP. 2020. Elevated ACE-2 expression in the olfactory neuroepithelium: implications for anosmia and upper respiratory SARS-CoV-2 entry and replication. Eur Respir J 56:2001948–2001922. https://doi.org/10.1183/13993003.01948-2020.

14. Hamming I, Timens W, Bulthuis MLC, Lely AT, Navis GJ, van Goor H. 2004. Tissue distribution of ACE2 protein, the functional receptor for SARS coronavirus. A first step in understanding SARS pathogenesis. J Pathol 203:631–637. https://doi.org/10.1002/path.1570.

15. Sungnak W, Huang N, Bécavin C, Berg M, Queen R, Litvinukova M, Talavera-López C, Maatz H, Reichart D, Sampaziotis F, Worlock KB, Yoshida M, Barnes JL, Banovich NE, Barbry P, Brazma A, Collin J, Desai TJ, Duong TE, Eickelberg O, Falk C, Farzan M, Glass I, Gupta RK, Haniffa M, Horvath P, Hubner N, Hung D, Kaminski N, Krasnow M, Kropski JA, Kuhnemund M, Lako M, Lee H, Leroy S, Linnarson S, Lundeberg J, Meyer KB, Miao Z, Misharin AV, Nawijn MC, Nikolic MZ, Noseda M, Ordovas-Montanes J, Oudit GY, Pe'er D, Powell J, Quake S, Rajagopal J, Tata PR, Rawlins EL, HCA Lung Biological Network, et al. 2020. SARS-CoV-2 entry factors are highly expressed in nasal epithelial cells together with innate immune genes. Nat Med 26:681–687. https://doi.org/10.1038/s41591-020-0868-6.

16. Singh M, Bansal V, Feschotte C. 2020. A single-cell RNA expression map of human coronavirus entry factors. Cell Rep 32:108175. https://doi.org/10.1016/j.celrep.2020.108175.

17. Bunyavanich S, Do A, Vicencio A. 2020. Nasal gene expression of angiotensin-converting enzyme 2 in children and adults. JAMA 323:2427–2429. https://doi.org/10.1001/jama.2020.8707.

18. Larrat S, Summa N. 2021. Ferret Mustela furo. Vet Clin North Am Exot Anim Pract 24:37–51. https://doi.org/10.1016/j.cvex.2020.09.001.

19. Monchatre-Leroy E, Lesellier S, Wasniewski M, Picard-Meyer E, Richomme C, Boué F, Lacôte S, Murri S, Pulido C, Vulin J, Salguero FJ, Gouilh MA, Servat A, Marianneau P. 2021. Hamster and ferret experimental infection with intranasal low dose of a single strain of SARS-CoV-2. J Gen Virol 102:001567. https://doi.org/10.1099/jgv.0.001567.

20. Ryan K, Bewley K, Fotheringham S, et al. 2021. Dose-dependent response to infection with SARS-CoV-2 in the ferret model and evidence of protective immunity. Nat Commun 12:81. https://doi.org/10.1038/s41467-020-20439-y.

21. Hou YJ, Chiba S, Halfmann P, Ehre C, Kuroda M, Dinnon KH, Leist SR, Schäfer A, Nakajima N, Takahashi K, Lee RE, Mascenik TM, Graham R, Edwards CE, Tse LV, Okuda K, Markmann AJ, Bartelt L, de Silva A, Margolis DM, Boucher RC, Randell SH, Suzuki T, Gralinski LE, Kawaoka Y, Baric RS. 2020. SARS-CoV-2 D614G variant exhibits efficient replication ex vivo and transmission in vivo. Science 370:1464–1468. https://doi.org/10.1126/science.abe8499.

22. Zhou B, Thao TTN, Hoffmann D, Taddeo A, Ebert N, Labroussaa F, Pohlmann A, King J, Steiner S, Kelly JN, Portmann J, Halwe NJ, Ulrich L, Trüeb BS, Fan X, Hoffmann B, Wang L, Thomann L, Lin X, Stalder H, Pozzi B, de Brot S, Jiang N, Cui D, Hossain J, Wilson MM, Keller MW, Stark TJ, Barnes JR, Dijkman R, Jores J, Benarafa C, Wentworth DE, Thiel V, Beer M. 2021. SARS-CoV-2 spike D614G

23. change enhances replication and transmission. Nature 592:122–127. https://doi.org/10.1038/s41586-021-03361-1.

23. Plante JA, Liu Y, Liu J, Xia H, Johnson BA, Lokugamage KG, Zhang X, Muruato AE, Zou J, Fontes-Garfias CR, Mirchandani D, Scharton D, Bilello JP, Ku Z, An Z, Kalveram B, Freiberg AN, Menachery VD, Xie X, Plante KS, Weaver SC, Shi PY. 2021. Spike mutation D614G alters SARS-CoV-2 fitness. Nature 592:116–121. https://doi.org/10.1038/s41586-020-2895-3.

24. Korber B, Fischer WM, Gnanakaran S, Yoon H, Theiler J, Abfalterer W, Hengartner N, Giorgi EE, Bhattacharya T, Foley B, Hastie KM, Parker MD, Partridge DG, Evans CM, Freeman TM, de Silva TI, Angyal A, Brown RL, Carrilero L, Green LR, Groves DC, Johnson KJ, Keeley AJ, Lindsey BB, Parsons PJ, Raza M, Rowland-Jones S, Smith N, Tucker RM, Wang D, Wyles MD, McDanal C, Perez LG, Tang H, Moon-Walker A, Whelan SP, LaBranche CC, Saphire EO, Montefiori DC. 2020. Tracking changes in SARS-CoV-2 spike: evidence that D614G increases infectivity of the COVID-19 virus. Cell 182:812–827. https://doi.org/10.1016/j.cell.2020.06.043.

25. Volz E, Hill V, McCrone JT, Price A, Jorgensen D, O'Toole Á, Southgate J, Johnson R, Jackson B, Nascimento FF, Rey SM, Nicholls SM, Colquhoun RM, da Silva Filipe A, Shepherd J, Pascall DJ, Shah R, Jesudason N, Li K, Jarrett R, Pacchiarini N, Bull M, Geidelberg L, Siveroni I, Goodfellow I, Loman NJ, Pybus OG, Robertson DL, Thomson EC, Rambaut A, Connor TR, Koshy C, Wise E, Cortes N, Lynch J, Kidd S, Mori M, Fairley DJ, Curran T, McKenna JP, Adams H, Fraser C, Golubchik T, Bonsall D, Moore C, Caddy SL, Khokhar FA, Wantoch M, Reynolds N, Warne B, et al. 2021. Evaluating the effects of SARS-CoV-2 spike mutation D614G on transmissibility and pathogenicity. Cell 184:64–75. https://doi.org/10.1016/j.cell.2020.11.020.

26. Hanson KE, Barker AP, Hillyard DR, Gilmore N, Barrett JW, Orlandi RR, Shakir SM. 2020. Self-collected anterior nasal and saliva specimens versus health care worker-collected nasopharyngeal swabs for the molecular detection of SARS-CoV-2. J Clin Microbiol 58:1–5. https://doi.org/10.1128/JCM.01824-20.

27. Zhou Y, O'Leary TJ. 2021. Relative sensitivity of anterior nares and nasopharyngeal swabs for initial detection of SARS-CoV-2 in ambulatory patients: rapid review and meta-Analysis. PLoS One 16:e0254559. https://doi.org/10.1371/journal.pone.0254559.

28. Wang X, Tan L, Wang X, Liu W, Lu Y, Cheng L, Sun Z. 2020. Comparison of nasopharyngeal and oropharyngeal swabs for SARS-CoV-2 detection in 353 patients received tests with both specimens simultaneously. Int J Infect Dis 94:107–109. https://doi.org/10.1016/j.ijid.2020.04.023.

29. Lee RA, Herigon JC, Benedetti A, Pollock NR, Denkinger CM, Scholar G. 2020. Performance of saliva, oropharyngeal swabs, and nasal swabs. J Clin Microbiol 59:e02881-20. https://doi.org/10.1128/JCM.02881-20.

30. Jones TC, Biele G, Mühlemann B, Veith T, Schneider J, Beheim-Schwarzbach J, Bleicker T, Tesch J, Schmidt ML, Sander LE, Kurth F, Menzel P, Schwarzer R, Zuchowski M, Hofmann J, Krumbholz A, Stein A, Edelmann A, Corman VM, Drosten C. 2021. Estimating infectiousness throughout SARS-CoV-2 infection course. Science https://doi.org/10.1126/science.abi5273.

31. Kim Y-I, Yu K-M, Koh J-Y, Kim E-H, Kim S-M, Kim EJ, Casel MA, Rollon R, Jang S-G, Song M-S, Park S-J, Jeong HW, Kim E-G, Lee O-J, Choi Y, Lee S-A, Park S-H, Jung JU, Choi YK. 2021. Age-dependent pathogenic characteristics of SARS-CoV-2 infection in ferrets. Res Sq https://doi.org/10.21203/rs.3.rs-131380/v2.

32. Laverack M, Tallmadge RL, Venugopalan R, Cronk B, Zhang XL, Rauh R, Saunders A, Nelson WM, Plocharczyk E, Diel DG. 2021. Clinical evaluation of a multiplex real-time RT-PCR assay for detection of SARS-CoV-2 in individual and pooled upper respiratory tract samples. Arch Virol 166:2551–2561. https://doi.org/10.1007/s00705-021-05148-1.

33. Palmer MV, Martins M, Falkenberg S, Buckley A, Caserta LC, Mitchell PK, Cassmann ED, Rollins A, Zylich NC, Renshaw RW, Guarino C, Wagner B, Lager K, Diel DG. 2021. Susceptibility of white-tailed deer (Odocoileus virginianus) to SARS-CoV-2. J Virol 95:e00083-21. https://doi.org/10.1128/JVI.00083-21.

34. Carvallo FR, Martins M, Joshi LR, Caserta LC, Mitchell PK, Cecere T, Hancock S, Goodrich EL, Murphy J, Diel DG. 2021. Severe SARS-CoV-2 infection in a cat with hypertrophic cardiomyopathy. Viruses 13:1510. https://doi.org/10.3390/v13081510.

35. Wong ML, Medrano JF. 2005. One-step versus two-step real. Biotechniques 39:75–85. https://doi.org/10.2144/05391RV01.